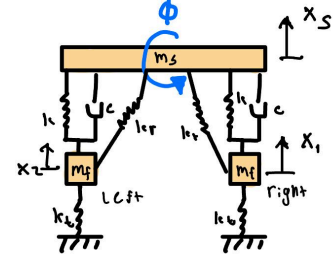


Half Car Model: Roll Response Analysis

The half-car model was derived using the front view of the car. The anti-roll bar was also to be considered with this model. Considering displacement of the three masses (M_s , M_f , M_f), newtons law of motion is used to describe the system and their states. Since this model has four degrees of freedom, four equations were derived to describe each degree of freedom:



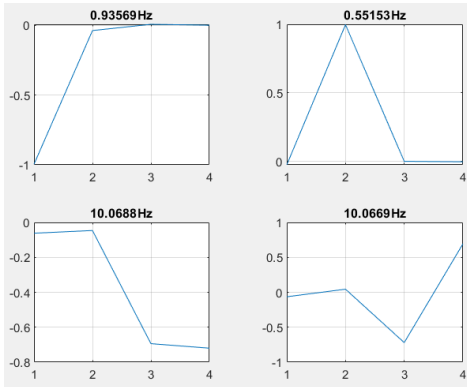
$$\begin{aligned}\ddot{x}_s &= [\ddot{x}_s [k_{t1} - k_{t2}] + \theta [a_{t1} l_{t1} + a_{t1} l_{t1}] + x_1 [k_{t1}] + x_2 [k_{t2}] + \ddot{x}_s [c_{t1} - c_{t2}] + \dot{\theta} [a_{t1} c_{t1} + a_{t1} c_{t1}] + \dot{x}_1 [c_{t1}] + \dot{x}_2 [c_{t2}]] \frac{1}{m_s} \\ \ddot{\theta} &= [\ddot{x}_s [-a_{t1} l_{t1} + a_{t1} l_{t1}] + \theta [k_{t1} a_{t1}^2 - k_{t2} a_{t2}^2] + x_1 [-a_{t1} l_{t1}] + x_2 [-a_{t2} l_{t2}] + \ddot{x}_s [-a_{t1} c_{t1} + a_{t1} c_{t1}] + \dot{\theta} [c_{t1} a_{t1}^2 - c_{t2} a_{t2}^2] + \dot{x}_1 [-a_{t1} c_{t1}] + \dot{x}_2 [-a_{t2} c_{t2}]] \frac{1}{I} \\ \ddot{x}_1 &= [\ddot{x}_s [k_{t1}] + \theta [-a_{t1} l_{t1}] + x_1 [-k_{t1} - k_{t1}] + x_2 [0] + \ddot{x}_s [c_{t1}] + \dot{\theta} [-a_{t1} c_{t1}] + \dot{x}_1 [-c_{t1} - c_{t1}] + \dot{x}_2 [0]] \frac{1}{m_f} \\ \ddot{x}_2 &= [\ddot{x}_s [k_{t2}] + \theta [a_{t2} l_{t2}] + x_1 [0] + x_2 [-k_{t1} - k_{t2}] + \ddot{x}_s [c_{t2}] + \dot{\theta} [a_{t2} c_{t2}] + \dot{x}_1 [0] + \dot{x}_2 [-c_{t1} - c_{t2}]] \frac{1}{m_f}\end{aligned}$$

Here we have four second-order differential equations that fully describe the system states. To model the system in MatLab the system of equations was converted into states space form: $Ax + Bu = x'$.

$$\begin{aligned}d_1 &= x_s & \dot{d}_1 &= \dot{x}_s & d_5 & \\ d_2 &= \theta & \dot{d}_2 &= \dot{\theta} & d_6 & \\ d_3 &= x_1 & \dot{d}_3 &= \dot{x}_1 & d_7 & \\ d_4 &= x_2 & \dot{d}_4 &= \dot{x}_2 & d_8 & \\ d_5 &= \dot{x}_s & \dot{d}_5 &= \ddot{x}_s & & \\ d_6 &= \dot{\theta} & \dot{d}_6 &= \ddot{\theta} & & \\ d_7 &= \dot{x}_1 & \dot{d}_7 &= \ddot{x}_1 & & \\ d_8 &= \dot{x}_2 & \dot{d}_8 &= \ddot{x}_2 & & \end{aligned}$$

$$\begin{aligned}\dot{d}_5 &= \ddot{x}_s = [d_1 [k_{t1} - k_{t2}] + d_2 [a_{t1} l_{t1} + a_{t1} l_{t1}] + d_3 [k_{t1}] + d_4 [k_{t2}] + d_5 [c_{t1} - c_{t2}] + d_6 [a_{t1} c_{t1} + a_{t1} c_{t1}] + d_7 [c_{t1}] + d_8 [c_{t2}]] \\ \dot{d}_6 &= \ddot{\theta} = [d_1 [-a_{t1} l_{t1} + a_{t1} l_{t1}] + d_2 [k_{t1} a_{t1}^2 - k_{t2} a_{t2}^2] + d_3 [-a_{t1} l_{t1}] + d_4 [-a_{t2} l_{t2}] + d_5 [-a_{t1} c_{t1} + a_{t1} c_{t1}] + d_6 [c_{t1} a_{t1}^2 - c_{t2} a_{t2}^2] + d_7 [-a_{t1} c_{t1}] + d_8 [-a_{t2} c_{t2}]] \\ \dot{d}_7 &= \ddot{x}_1 = [d_1 [k_{t1}] + d_2 [-a_{t1} l_{t1}] + d_3 [-k_{t1} - k_{t1}] + d_4 [0] + d_5 [c_{t1}] + d_6 [-a_{t1} c_{t1}] + d_7 [-c_{t1} - c_{t1}] + d_8 [0]] \\ \dot{d}_8 &= \ddot{x}_2 = [d_1 [k_{t2}] + d_2 [a_{t2} l_{t2}] + d_3 [0] + d_4 [-k_{t1} - k_{t2}] + d_5 [c_{t2}] + d_6 [a_{t2} c_{t2}] + d_7 [0] + d_8 [-c_{t1} - c_{t2}]]\end{aligned}$$

$$\begin{bmatrix} \dot{d}_1 \\ \dot{d}_2 \\ \dot{d}_3 \\ \dot{d}_4 \\ \dot{d}_5 \\ \dot{d}_6 \\ \dot{d}_7 \\ \dot{d}_8 \end{bmatrix} = \begin{bmatrix} 0 & 0 & 0 & 0 & 1 & 0 & 0 & 0 \\ 0 & 0 & 0 & 0 & 0 & 1 & 0 & 0 \\ 0 & 0 & 0 & 0 & 0 & 0 & 1 & 0 \\ 0 & 0 & 0 & 0 & 0 & 0 & 0 & 1 \\ \frac{[k_{t1} - k_{t2}]}{m_s} & \frac{[a_{t1} l_{t1} + a_{t1} l_{t1}]}{m_s} & \frac{[k_{t1}]}{m_s} & \frac{[k_{t2}]}{m_s} & \frac{[c_{t1} - c_{t2}]}{m_s} & \frac{[a_{t1} c_{t1} + a_{t1} c_{t1}]}{m_s} & \frac{[c_{t1}]}{m_s} & \frac{[c_{t2}]}{m_s} \\ \frac{[-a_{t1} l_{t1} + a_{t1} l_{t1}]}{I} & \frac{[k_{t1} a_{t1}^2 - k_{t2} a_{t2}^2]}{I} & \frac{[-a_{t1} l_{t1}]}{I} & \frac{[-a_{t2} l_{t2}]}{I} & \frac{[-a_{t1} c_{t1} + a_{t1} c_{t1}]}{I} & \frac{[c_{t1} a_{t1}^2 - c_{t2} a_{t2}^2]}{I} & \frac{[-a_{t1} c_{t1}]}{I} & \frac{[-a_{t2} c_{t2}]}{I} \\ \frac{[k_{t1}]}{m_f} & \frac{[-a_{t1} l_{t1}]}{m_f} & \frac{[-k_{t1} - k_{t1}]}{m_f} & \frac{[0]}{m_f} & \frac{[c_{t1}]}{m_f} & \frac{[-a_{t1} c_{t1}]}{m_f} & \frac{[-c_{t1} - c_{t1}]}{m_f} & \frac{[0]}{m_f} \\ \frac{[k_{t2}]}{m_f} & \frac{[a_{t2} l_{t2}]}{m_f} & \frac{[0]}{m_f} & \frac{[-k_{t1} - k_{t2}]}{m_f} & \frac{[c_{t2}]}{m_f} & \frac{[a_{t2} c_{t2}]}{m_f} & \frac{[0]}{m_f} & \frac{[-c_{t1} - c_{t2}]}{m_f} \end{bmatrix} \begin{bmatrix} d_1 \\ d_2 \\ d_3 \\ d_4 \\ d_5 \\ d_6 \\ d_7 \\ d_8 \end{bmatrix} + \begin{bmatrix} 0 & 0 \\ 0 & 0 \\ 0 & 0 \\ 0 & 0 \\ \frac{k_{t1} b}{m_1} & 0 \\ 0 & \frac{k_{t2} b}{m_2} \\ 0 & 0 \\ 0 & 0 \end{bmatrix} \begin{bmatrix} x_1 \\ x_2 \end{bmatrix}$$



Using the parameters from problem 6 on page 880, matrix (A) was used to calculate the Eigen vectors and Eigen values. The system reads as partially stable since damping coefficients are set to zero. The system's natural frequency was obtained through the Eigenvalues of matrix A: Natural Frequencies = $[0.93569, 0.55153, 10.0688, 10.0669]$. There is a correlated natural frequency per degree of freedom. The corresponding mode shapes for $K_r = 0$ are shown.

Similarly, the natural frequencies and mode shapes of the system for $K_r = 10000 \text{ N m/rad}$ and $K_r = 50000 \text{ N m/rad}$ are shown:

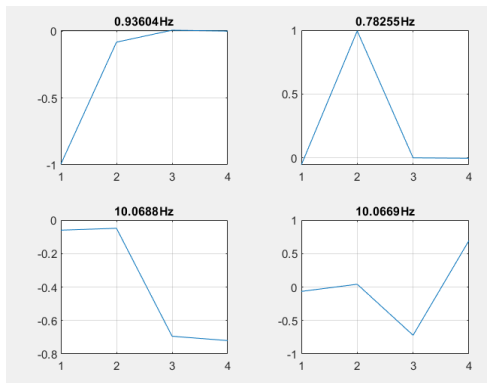


Figure: ($K_r = 10000 \text{ N m /rad}$)

Natural Frequencies = $[0.93604, 0.78255, 10.0688, 10.0669]$

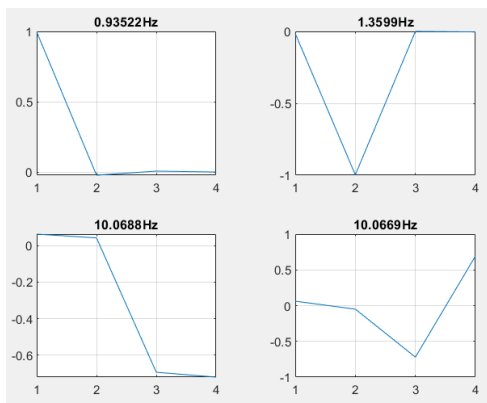
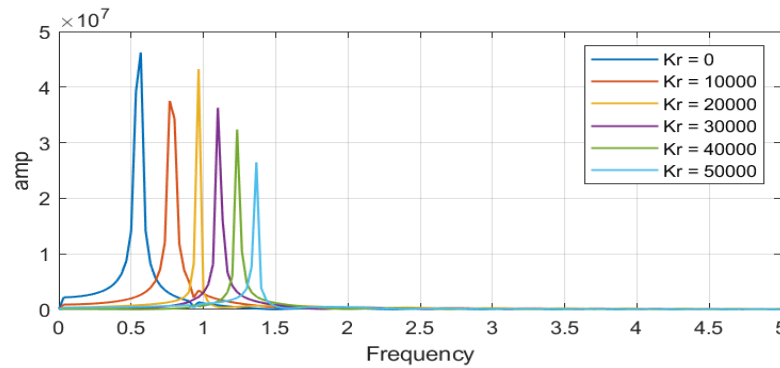


Figure: ($K_r = 50000 \text{ N m /rad}$)

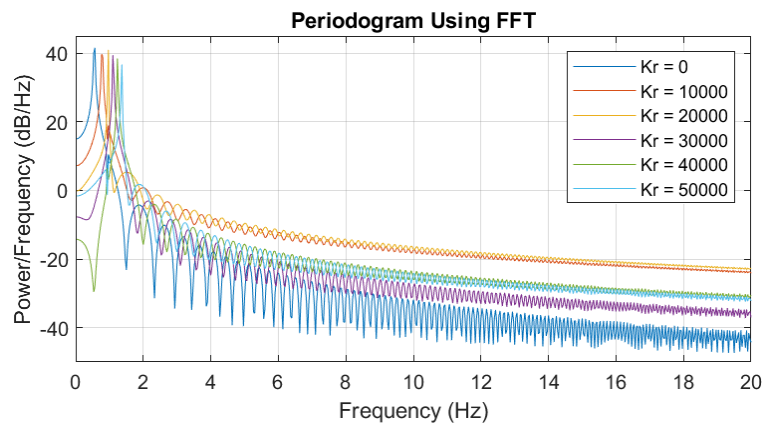
Natural Frequencies = $[0.93522, 1.3599, 10.0688, 10.0668]$

Here we see that the anti-roll bar stiffness affects only the roll mode's natural frequencies. The roll mode material frequency increases as stiffness increases.

Diving deeper into how the system's roll mode changes with increasing stiffness. The system was given road inputs of a swept sin wave. This swept sin wave inherently introduces every frequency input within the natural frequency range. The Fast Fourier Transform was computed using the roll response of the system given the road inputs. With varying rolling stiffness we can see how the roll mode shifts.



The FFT shows the rolling response natural frequency shifting to higher natural frequencies as rolling stiffness increases in increments of 10,000 N m/rad. The frequencies span from about 0.5 Hz - 1.4 Hz. The rolling natural frequency seems to have a linear response to increasing Kr values. To get a closer analysis of the response to varying rolling stiffness the power spectral density is to be considered to analyze the power of total response through the span of 0 Hz - 20 Hz. This allows us to see in more depth the effects of other frequencies on the system rather than just the natural response.



Given the same conditions, we can see that the power spectral density shows us how the varying rolling stiffness not only affects the roll natural frequencies but also the settling response at the limit. Taking a look at the higher-frequency responses we see that as kr increases, the high-frequency response will operate within a power range of 20-45 dB/Hz.

By matching the rolling frequency to the bounce frequency we can obtain the four mode shapes that correlate to the natural frequency of the system.

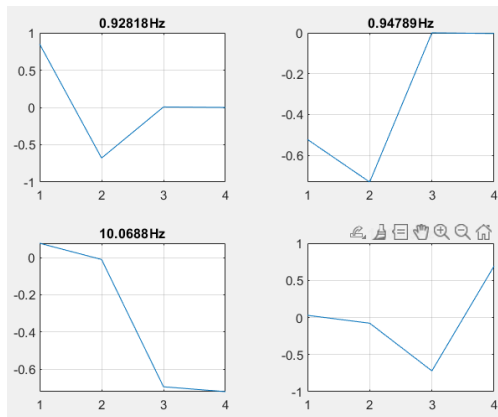
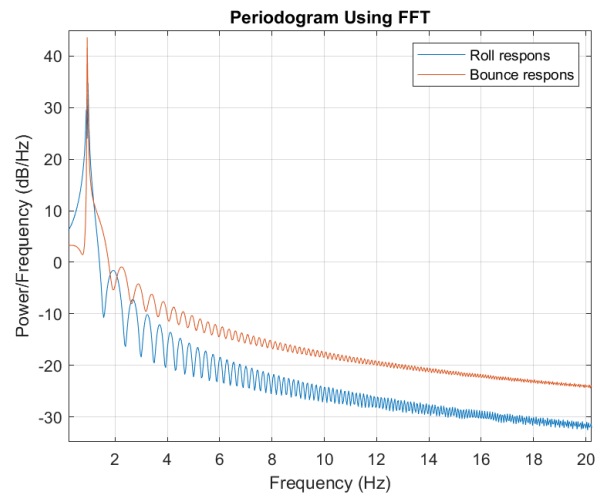
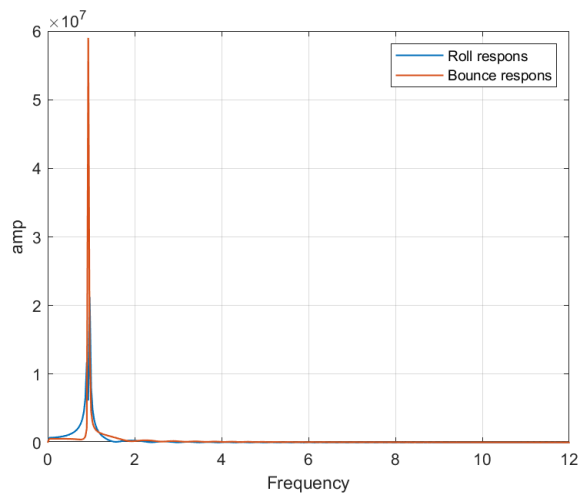


Figure: Here an anti-roll bar stiffness of 18790 N m/rad was used to obtain the same resident frequency as the bounce response.

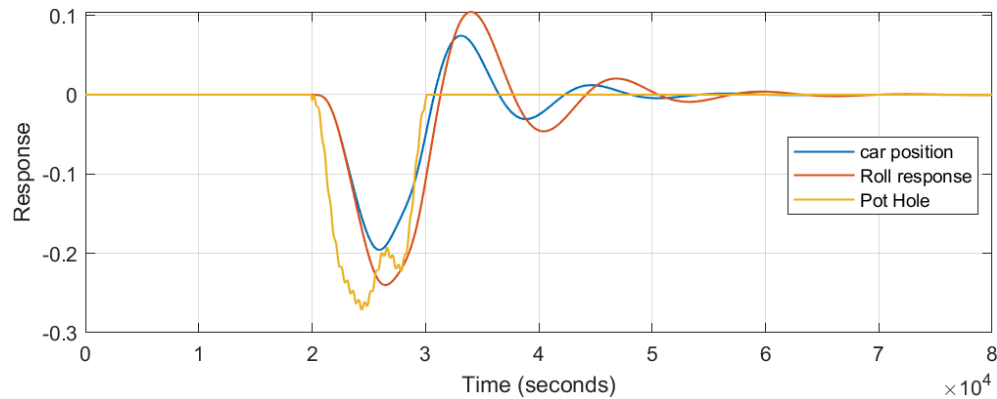
Similarly, we can look at the Fast Fourier Transform and the power spectral density of the bounce and roll response given a swept sine wave road input.



Here we can see that when we set the anti-roll bar stiffness to 18790 N m/rad the roll response and bounce response natural frequency are the same. Taking a look at the power spectral density we can see that bounce response at higher frequencies is less damped since the bounce has a faster settling time.

Furthermore, we can continue to analyze the roll response given a different input. We previously used a swept sin wave as input to introduce frequencies within the band of the system's natural frequencies to analyze the magnitude of the roll response. Now we can introduce a new impulsive response to see how the system will react.

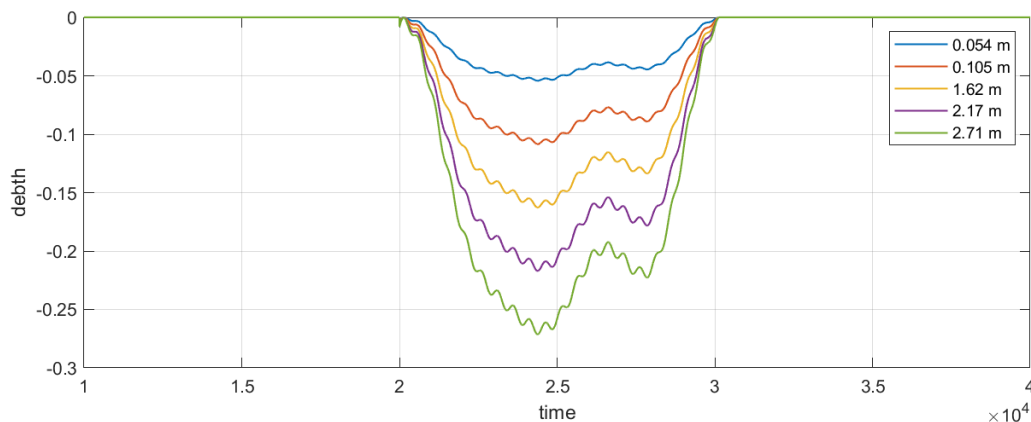
For this analysis, we are going to assume the car is traveling at a speed of 10 m/s, over a road profile with a pot hole of base length 1 meter and depth of 0.271m. If we assume that one tire interacted with the pothole and the other is maintained on a smooth flat road, the system's roll and bounce responses are shown as a function of time.



The bounce response is in meters while the roll response is in radians. The damping coefficients used for this model were 1000 N s/m. Here the pothole strikes at $t=2$ s and spans until $t=3$ s. We can see that both the system's roll and bounce response have a delayed response to the impulsive road profile. From observations, we can also see that the bounce has a slightly faster settling time than the roll. We can approximate the settling time for the bounce to be 5 seconds while the roll settling time is about 5.5 seconds. The settling time is inversely proportional to the damping coefficient up to the system's critical damping.

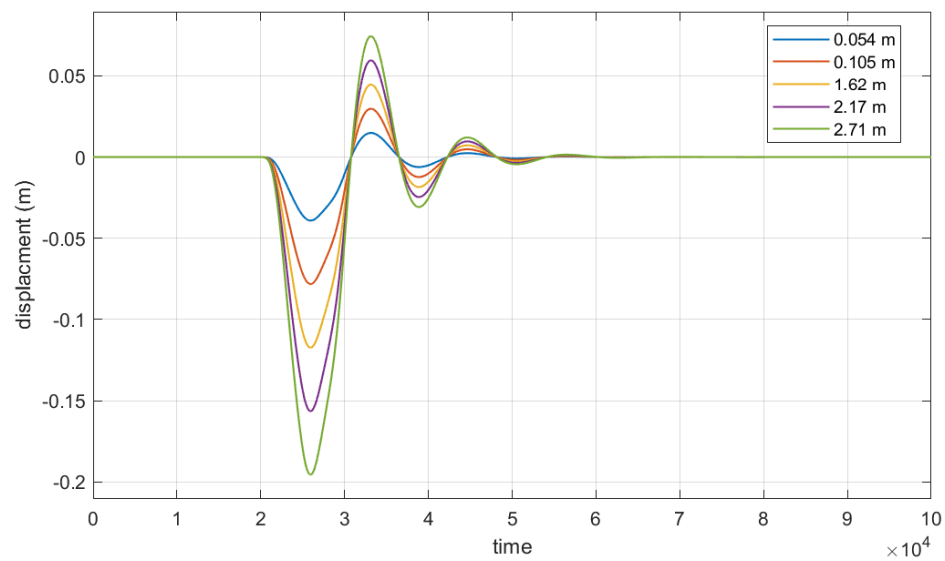
We can vary the whole depth to see how this will affect the roll and bounce response. Here are the outcomes:

Road Profile

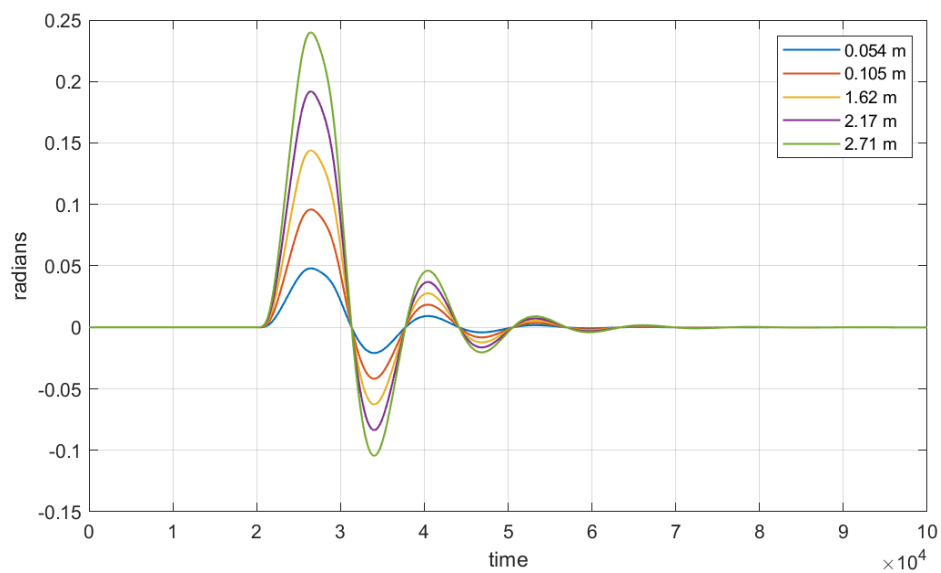


System response:

Bounce response



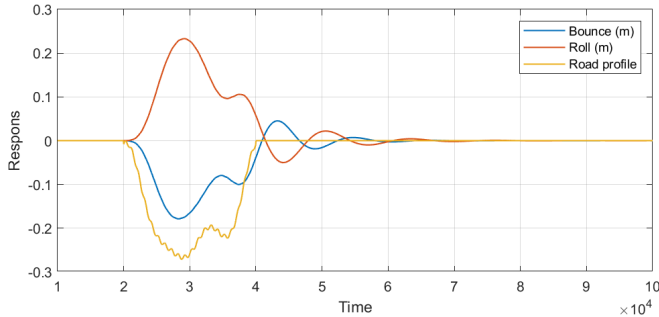
Roll response



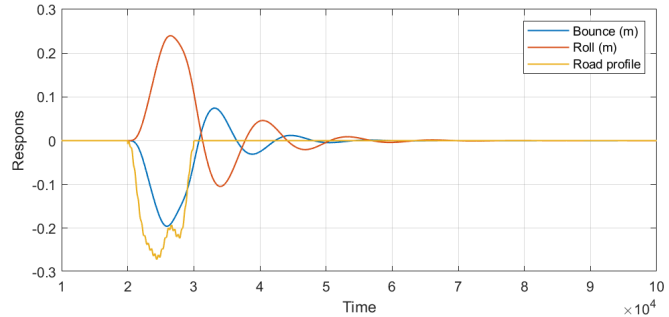
The road profile for the pot whole was flipped to the other tire. We see that having a pothole with less depth decreases the amplitude and settling time for both responses.

Instead of varying the depth of the pothole, we can also investigate the systems response to varying pothole length with a constant depth. Here are the outcomes :

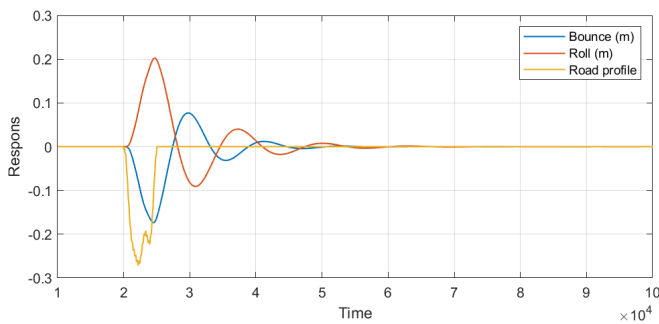
Length = 2m



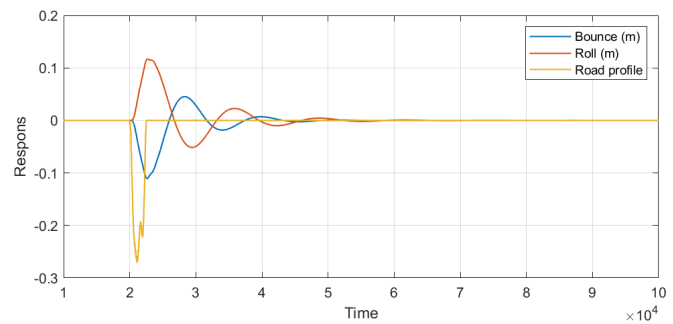
Length = 1m



Length = 0.5 m

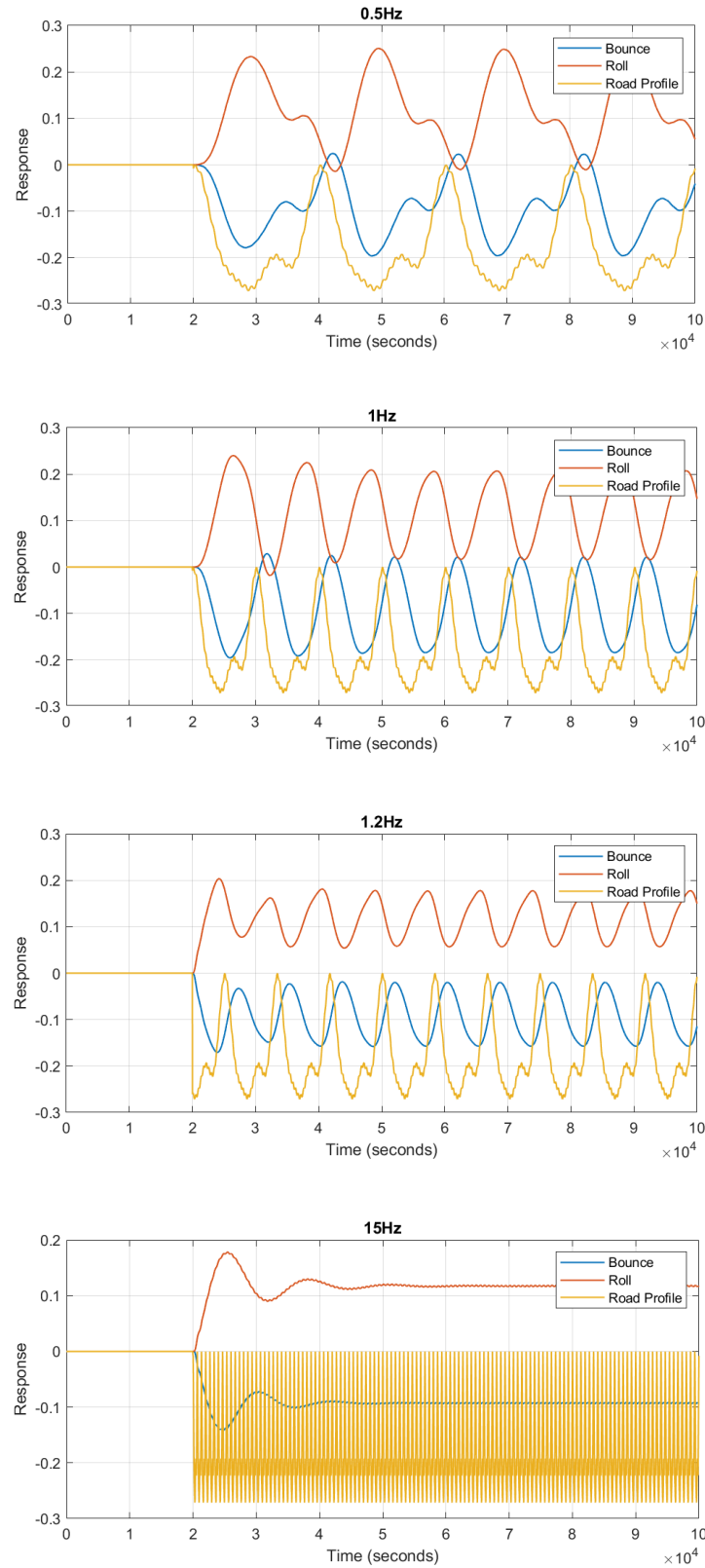


Length = 0.25 m



The responses show varying pothole lengths with a constant pothole depth. Taking a look at the response for a pothole of length 2 meters, we see that the system is given enough time to respond to the small inner bump inside the pothole. But in every other response, we see that the system is almost fully neglecting the inner bump. This is because for the smaller lengths the system will still be reacting to the impulsive drop at $t = 2$ by the time the small bump occurs. We can also see that the magnitude of the response will decrease as the length of the pothole gets smaller. This is because at higher frequencies the response is dampened by the fundamental delay of the system. As a result of the magnitude dropping with decreasing pothole length, we see a decrease in settling time as well.

Lastly, we can take a look at the car's response to an increase in pothole frequency. The pothole depth will be kept constant for this analysis. The responses are shown:



As expected we see that as the frequency of the pothole increases the oscillatory response of the system dampens. This is because the system has a settling time. If the system experiences an input before the system is settled then the past responses become superimposed with the current response. At the limit, the pothole frequency goes to infinity. The impulse of the pothole will simulate a constant force and moment acting on the system that is proportional to the average depth of the pothole.

Parameters:

```
ms=1085/2
m1 = 40
m2 = 40
k1 = 10000
k2 = 10000
c1 = 1000
c2 = 1000
k1t = 150000
k2t = 150000
a1 = 0.7
a2 = 0.75
I = 820
kr = [0 10000 50000 18790]
```

Simulink Model:

